Food Chemistry: X 21 (2024) 101004

Contents lists available at ScienceDirect

Food Chemistry: X

journal homepage: www.sciencedirect.com/journal/food-chemistry-x

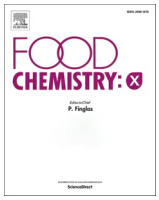

Physicochemical changes and *in vitro* digestibility of three banana starches at different maturity stages

Jiashui Wang [a,1,*], Yanxia Li [a,1], Weihong Ma [a,1], Jiali Zhang [a], Hongbin Yang [a], Peicong Wu [a], Jingyang Li [a], Zhiqiang Jin [b]

[a] *Tropical Crops Genetic Resources Institutes, Haikou Experimental Station, Chinese Academy of Tropical Agricultural Sciences, Key Laboratory of Crop Gene Resources and Germplasm Enhancement in Southern China, Ministry of Agriculture and Rual Affairs, Haikou, 571101, China*

[b] *Sanya Research Institute of Chinese Academy of Tropical Agricultural Sciences, Sanya 572024, China*

ARTICLE INFO

Keywords:
Banana starch
Degree of ripeness
Morphology
Physicochemical properties
Digestibility

ABSTRACT

This study aimed to compare the changes in physicochemical properties of the starch isolated from three banana cultivars (*Musa* AAA group, *Cavendish* subgroup; *Musa* ABB group, *Pisang Awak* subgroup; *Musa* AA group, *Huangdijiao* subgroup) at five different maturity stages. The results revealed both similarities and significant differences in micromorphology and physicochemical characteristics of the three banana varieties during different growth stages. Apparent amylose content and particle size of the three starches increased with the ripeness of banana. Light microscopy and scanning electron microscopy revealed that starch particles of the three starches had different microscopic characteristics, and that banana starch morphology was basically unchanged at various growth stages. Moreover, the pasting and thermal properties of the banana starches were significantly different at various growth stages. The resistant starch content of the three banana cultivars was about 80% at all growth stages. *Musa* AAA group, *Cavendish* subgroup had the highest resistant starch content at stage V. This study provides insights into the starch changes of three banana cultivars during ripening.

Introduction

Starch, a well-studied carbohydrate polymer, is mainly composed of amylose and amylopectin. According to its *in vivo* digestibility, starch can be classified into rapidly digestible starch (RDS), slowly digestible starch (SDS) and resistant starch (RS) (Gutiérrez & Tovar, 2021). An increasing number of studies have suggested the health-promoting effects of RS, such as lowering postprandial blood glucose levels and functioning as prebiotics (Das, Rajan, Biswas, & Banerjee, 2022). With the rising healthcare awareness of the public, food practitioners have been seeking a stable source of RS for a long time. In this respect, green bananas stand out for their high RS contents (Kaur, Dhull, Kumar, & Singh, 2020; Wang, Wang, Ma, Xu, Zang, Tan, et al., 2019). The banana has been widely cultivated in the tropical and subtropical area. In recent decades, banana starch (BS) has attracted a lot of attention owe to its commercial competitive potential and functional features in terms of human well-being (Kaur, Dhull, Kumar, & Singh, 2020; Zhang, Whistler, BeMiller, & Hamaker, 2005). These studies involved production, physicochemical properties (including native and modified starch), and digestibility of BS.

Studies have shown that starch characteristics are different at various harvest periods. Studies have also shown that cassava (Tan, Gu, Li, Xie, Chen, & Zhang, 2017), potato (Madsen & Christensen, 1996), yam (Huang, Lin, & Wang, 2006), taro (Himeda, Yanou, Nguimbou, Gaiani, & Mbofung, 2012), water caltrop (Chiang, Li, Huang, & Wang, 2007), sago palms (Tie, Karim, & Manan, 2010) starches have different physicochemical characteristics at various plant physiological stages. For instance, a study found that the average granule size, peak viscosity, and breakdown of potato starch were increased at a late harvest period; in contrast, gelatinization temperatures and amylose content were slightly decreased with late harvest; gelatinization enthalpy, on the other hand, was not affected (Noda, Tsuda, Mori, Takigawa, Matsuura-Endo, Saito, et al., 2004). In terms of BS, the morphology, structure, physiochemical and digestibility characteristics vary with banana cultivars, regional climatic conditions and harvest periods (Bello-Pérez, Agama-Acevedo, Sánchez-Hernández, & Paredes-López, 1999; Srikaeo, Mingyai, & Sopade, 2011; Utrilla-Coello, Rodríguez-Huezo, Carrillo-Navas, Hernández-Jaimes, Vernon-Carter, & Alvarez-Ramirez, 2014).

* Corresponding author.
[1] These authors contributed equally to this study.

https://doi.org/10.1016/j.fochx.2023.101004
Received 5 July 2023; Received in revised form 7 November 2023; Accepted 10 November 2023
Available online 11 November 2023

The RS content of BS was also significantly affected by postharvest storage conditions (Wang, Tang, Chen, & Huang, 2014). However, to the best of our knowledge, no study has reported on the physicochemical properties of banana starch at various maturity stages.

China is not only a major banana producer, but a major banana consumer in the world. The three dominant banana cultivars in China are *Musa* AAA group, *Cavendish* subgroup (MC), *Musa* ABB group, *Pisang Awak* subgroup (MP), and *Musa* AA group, *Huangdijiao* subgroup (MH), which are widely grown in Hainan Province. A better understanding of the structure and physiochemical characteristics of banana starch from the three cultivars at different maturity stages can improve the development of banana industry in China. Therefore, this study aimed to examine the physicochemical and *in vitro* digestibility of the starch from the three banana cultivars at five different maturity stages. Apparent amylose content, particle size, chemical structure, crystallinity, thermal and pasting characteristics, and *in vitro* digestibility were analyzed to distinguish differences between the starches. The effect of cultivars and growth stages on the physicochemical and *in vitro* digestibility was investigated, and the correlation about the structure characteristics, apparent amylose content, and digestibility of the BS starch was also analyzed. Our results indicated that the physicochemical and *in vitro* digestibility of BS are correlated with both cultivars and growth stages. The results are of great significance to the application of different types of BS in food industry.

Materials and methods

Materials

Three banana varieties (MC, MP, and MH) grown at the banana experimental base of Chinese Academy of Tropical Agricultural Sciences (CATAS), in Danzhou (Hainan) of China were used in this study. The growth period of each variety was divided into five maturity stages after bud cut (MC: 12 (I), 24 (II), 36 (III), 48 (IV) and 60 (V) days; MP: 15 (I), 30 (II), 45 (III), 60 (IV) and 75 (V) days; MH: 5 (I), 10 (II), 15 (III), 20 (IV) and 25 (V) days). The bananas were harvested and stored at 25 °C for 24 h before starch isolation. All chemicals used in this study were of ACS-certified grade.

Bananas starch isolation

Bananas were peeled, sliced, and immersed in an acid solution containing citric acid (0.2 %, w/w) and ascorbic acid (0.02 %, w/w) at room temperature for 30 min. The samples were then dried in a vacuum oven at 45 °C for 24 h, crushed and sieved through a 100 mesh sieve to obtain banana flours. Starches were isolated from the flours via a water-alkaline extraction process as previously described (Cheng, Yang, Wang, Bing, Bao, Wen, et al., 2008).

Apparent amylose content

Iodine colorimetry was used to determine the apparent amylose content in BS via the modified AACC (1983) method 61–03 (10) (AACC, 1983). BS (10 mg) was mixed with 1 mL of anhydrous ethanol and 9 mL NaOH aqueous solution (1 M), and then stirred at 100 ℃ for 10 min. Distilled water was added to make up the volume to 500 mL. The obtained solution (25 mL) was then mixed with 0.5 mL acetic acid solution (1 M) and 0.5 mL iodine solution (0.2 %, w/w). The absorbance of amylose-iodine complex was measured at 620 nm.

Morphological and particle size analyses

Light microscopy

A light microscope (Olympus BX-51, Tokyo, Japan) was used for light microscopy analyses. A drop of starch suspension (1 %, w/w) was placed on a microscope slide that was then covered with a coverslip. The samples were observed under both normal light and polarized light. Images were taken at 40 × magnification.

Scanning electron microscopy (SEM)

A scanning electron microscope (model TM 3000, Hitachi, Japan) was used for microscopic examinations of the starch surface. Starch granules were put on an aluminum stub using double-sided adhesive tape and then vacuum-coated with gold (20 nm). Images were taken at 500 × magnification with an accelerating voltage of 10.00 kV.

Starch particle size measurement

A Malvern Mastersizer 3000 laser diffraction size analyzer (Malvern Instruments, Malvern, UK) was used to determine particle size and size distribution of the starches as previously described (Tan, Gu, Li, Xie, Chen, & Zhang, 2017). The values obtained for each sample were analyzed using Mastersizer software, which yielded the average granule diameter derived from the volume distribution (D [4,3]), the ratio of the volume of particles to the total surface area (D [3,2]), and a table showing the percentage of size distribution. Each sample was analyzed in triplicate.

X-ray diffraction (XRD) pattern

Crystalline structures of the starches were analyzed via a D/Max-2200 X-ray diffractometer (Rigaku Denki Co., Tokyo, Japan) with Cu Kα radiation at 44 kV and 26 mA. Samples were scanned from 4° to 40° (2θ) at a rate of 5°/min. Relative crystallinity was estimated according to the method described by Nara et al (Nara, Sakakura, & Komiya, 1983).

Fourier transform infrared spectroscopy (FT-IR)

Vector 33 Fourier transform infrared spectrophotometer (Bruker Company, Ettlingen, Germany) was used for structural analysis via an attenuated total reflection method. Starch was mixed with KBr (1:99), compressed to a sheet and scanned from 4000 to 400 cm^{-1} with the resolution of 4 cm^{-1}.

Differential scanning calorimetry (DSC) analysis

A thermal analysis software (Pyriswindow) and differential scanning calorimeter (DSC 8000, Perkin Elmer, Norwalk, Connecticut, USA) was used for thermal properties analysis. Starch (3 mg) was mixed with distilled water (7 mg) in stainless high-pressure pans, which were sealed and equilibrated at room temperature for 12 h. Samples were heated from 30 to 130 °C at 10 °C/min. The flow rate of N_2 was 20 mL/s. Gelatinization onset temperature (T_o), conclusion temperature (T_c), peak temperature (T_p), gelatinization range (ΔT), and enthalpy (ΔH) were measured.

Pasting properties

A Micro Visco-Amylo-Graph (Brabender, Germany) was used to measure the viscosity of the starches. Starch slurries (6 %, w/v) were prepared for the measurement. The measuring torque was 700 cmg. The slurries were heated from 30 to 95 °C at 7.5 °C/min, held at 95 °C for 5 min, cooled to 50 °C at 7.5 °C/min, and held at 50 °C for another 5 min.

In vitro digestion analysis

The digestibility was assessed using the method described by Englyst, Kingman, & Cummings (1992) with slight modifications. Fresh enzyme solution was prepared by adding 2 g pancreatin (8 USP) into 6.7 mL sodium acetate buffer (0.2 M, pH 5.2). The solution was then centrifuged at 4500 rpm for 10 min to obtain supernatant, which was mixed with 0.67 mL amyloglucosidase (300 U/mL).

Starch (300 mg) was added into 15 mL sodium acetate buffer (0.2 M,

pH 5.2) to form a suspension, followed by the addition of the above enzyme solution (0.75 mL) and incubation at 37 °C with continuous shaking (170 rpm) to initiate the hydrolysis. Aliquot (0.1 mL) of hydrolyzed solutions were taken at 20 and 120 min, and then mixed with 3 mL of 90 % ethanol immediately to deactivate the enzyme. The solution was centrifuged at 4500 rpm for 5 min to obtain supernatant, where the glucose content was determined by glucose oxidase/peroxidase (GOPOD) assay kit. The percentage of hydrolyzed starch was calculated by multiplying the glucose content by 0.9 (molar mass conversion from glucose to anhydroglucose). The RDS, SDS, and RS contents were calculated with the following formula:

$$RDS(\%) = [0.9 \times (G20 - FG)]/TS \quad (1)$$

$$SDS(\%) = [0.9 \times (G120 - G20)]/TS \quad (2)$$

$$RS(\%) = 1 - RSD(\%) - SDS(\%) \quad (3)$$

where G20 and G120 indicate the amount of glucose released at 20 min and at 120 min, respectively; FG represents the free glucose content; and TS is the total starch content.

Statistical analysis

Mean values and standard deviations were analyzed and reported by the Origin Program 8.0 (Origin Lab Company, USA). To estimate the effect of cultivars and growth stages on apparent amylose content, particle size, gelatinization temperature, enthalpy of gelatinization and pasting characteristics, a two-way analysis of variance (ANOVA) was performed using SPSS 26.0 Statistical Software Program (SPSS Inc., Chicago, United States). The correlation between the properties of the samples was analyzed by the Pearson product-difference correlation coefficient of SPSS.

Results and discussion

Apparent amylose content

Apparent amylose content is one of the main factors that affect the physicochemical properties of starch, such as rheological, gelatinization, retrogradation, and pasting properties (Baik & Lee, 2003). Besides, the apparent amylose content varies at various growth periods (Huang, Lin, & Wang, 2006). Therefore, the apparent amylose content of MC, MP, MH starches at different growth periods were determined (Table 1). The apparent amylose content increased from 20.26 % to 35.78 % for MC, from 22.91 % to 40.44 % for MP, and from 22.85 % to 36.18 % for MH as the bananas progressively matured. Interestingly, the MP starch had the highest apparent amylose content (40.44 %) at stage V and had the highest increase as growth progressed, which suggested that different varieties have different characteristics in starch accumulation. This is probably because of the different activities of the enzymes responsible for starch biosynthesis during banana growth and development (Tsai, Salamini, & Nelson, 1970). While consistent with the report of Thanyapanich, Jimtaisong, & Rawdkuen (2021) who detected lower apparent amylose content in *Musa* AAA starch than that in *Musa* ABB starch. Moreover, not all species amylose content that increased with maturity, as was found in the study of Bi, Zhang, Gu, Cheng, Li, Li, et al. (2019) that the apparent amylose content of plantain starch was unchanged before stage V and was significantly decreased at stage VII.

Table 1
Amylose content and granule diameter value of MC, MP and MH starches at different maturity stages (I-V). Data are reported as mean ± S. D. ($n = 3$).

Samples		Apparent amylose content (%)	*D* [4, 3]	*D* [3, 2]	*D* [V, 0.1]	*D* [V, 0.5]	*D* [V, 0.9]
MC	I	20.26 ± 1.30 ^{Ad}	33.63 ± 1.18 ^{Ca}	21.63 ± 0.21 ^{Ad}	12.57 ± 0.23 ^{Ae}	27.66 ± 0.06 ^{Ac}	57.23 ± 0.90 ^{Bd}
	II	22.56 ± 0.98 ^{Ad}	32.33 ± 0.06 ^{Ca}	23.73 ± 0.38 ^{Ac}	15.37 ± 0.32 ^{Ac}	30.33 ± 0.15 ^{Ac}	53.13 ± 0.40 ^{Bd}
	III	26.36 ± 1.30 ^{Ac}	38.80 ± 0.44 d ^{Cb}	25.37 ± 0.06 ^{Ac}	15.46 ± 0.05 ^{Ad}	32.57 ± 0.05 ^{Ac}	65.83 ± 0.28 ^{Bc}
	IV	30.38 ± 0.65 ^{Ab}	36.43 ± 0.32 ^{Cc}	26.73 ± 0.06 ^{Ab}	19.16 ± 0.11 ^{Aa}	34.93 ± 0.05 ^{Ab}	57.10 ± 0.50 ^{Bb}
	V	35.78 ± 0.49 ^{Aa}	54.10 ± 1.40 ^{Bd}	37.10 ± 0.36 ^{Aa}	20.10 ± 0.10 ^{Ab}	50.70 ± 0.62 ^{Aa}	152.00 ± 4.02 ^{Ba}
MP	I	22.91 ± 2.44 ^{Bd}	31.97 ± 1.46 ^{Ba}	25.67 ± 0.71 ^{Ad}	15.31 ± 0.15 ^{Be}	28.13 ± 0.57 ^{Bc}	58.83 ± 4.40 ^{Bd}
	II	32.51 ± 4.96 ^{Bd}	33.90 ± 0.65 ^{Ba}	23.67 ± 1.52 ^{Ac}	14.80 ± 0.20 ^{Bc}	28.40 ± 0.17 ^{Bc}	58.36 ± 1.85 ^{Bd}
	III	38.54 ± 0.33 ^{Bc}	36.83 ± 0.52 ^{Bb}	22.63 ± 0.06 ^{Ac}	13.22 ± 0.02 ^{Bd}	28.00 ± 0.10 ^{Bc}	75.00 ± 1.73 ^{Bc}
	IV	39.34 ± 0.65 ^{Bb}	43.93 ± 0.42 ^{Bc}	33.10 ± 0.01 ^{Ab}	19.50 ± 0.01 ^{Ba}	36.23 ± 0.05 ^{Bb}	76.16 ± 0.23 ^{Bb}
	V	40.44 ± 1.38 ^{Ba}	59.53 ± 1.09 ^{Bd}	29.37 ± 0.35 ^{Aa}	13.93 ± 0.15 ^{Bb}	44.23 ± 0.95 ^{Ba}	126.33 ± 2.51 ^{Ba}
MH	I	22.85 ± 0.03^{Cd}	33.62 ± 0.35 ^{Aa}	19.93 ± 0.06 ^{Bd}	11.90 ± 0.01 ^{Ce}	24.57 ± 0.11 ^{Bc}	56.80 ± 0.17 ^{Ad}
	II	30.09 ± 0.08^{Cd}	39.93 ± 2.10 ^{Aa}	22.26 ± 1.18 ^{Bc}	11.67 ± 0.23 ^{Cc}	25.80 ± 0.26 ^{Bc}	72.30 ± 6.53 ^{Ad}
	III	30.78 ± 0.24 ^{Cc}	46.37 ± 2.43 ^{Ab}	23.27 ± 0.05 ^{Bc}	11.80 ± 0.01^{Cd}	26.96 ± 0.05 ^{Bc}	108.00 ± 1.02 ^{Ac}
	IV	35.44 ± 0.81 ^{Cb}	58.11 ± 5.26 ^{Ac}	21.43 ± 0.23 ^{Bb}	11.26 ± 0.06 ^{Ca}	24.13 ± 0.23 ^{Bb}	92.57 ± 7.55 ^{Ab}
	V	36.18 ± 0.73 ^{Ca}	75.66 ± 9.83 ^{Ad}	29.40 ± 1.21 ^{Ba}	12.20 ± 0.17 ^{Cb}	61.80 ± 6.58 ^{Ba}	129.33 ± 11.50 ^{Aa}

Values in the same column with different superscripts represent significant difference ($P < 0.05$). Upper case letters represent ANOVA for cultivars, lower case letters represent ANOVA for growth stages.
[A]D [4, 3] is the average granule diameter derived from the volume distribution.
[B]D [3, 2] is the ratio of the volume of particles to the total surface area.
[C]D [V, 0.1] is the median of 10% granule diameter (μm).
[D]D [V, 0.5] is the median of 50% granule diameter (μm).
[E]D [V, 0.9] is the median of 90% granule diameter (μm).

Morphology observation and particle size distribution

Surface morphology

Normal light and polarized light microscopic results are shown in Fig. 1. Most MC and MH starch granules were oval while some granules displayed spindle-like shapes. In comparison, MP starch particles were mostly round with part of them being triangular. A maltese cross appeared at the top and edges of all the starch particles. This stems from the birefringent characteristic since starch is alternately stacked with semi-crystalline and amorphous regions (Sivak & Preiss, 1998).

The scanning electron microscopic images of MC, MP, and MH starches are shown in Fig. 2. It was found that both MC and MP starch granules had trigonal and pentagonal shape, and MH starches owned extra elongated ellipsoidal particles. The shape of MC starch granules changed with growth periods: MC granules were olivary and small at stage I, and became virgulate and large at stage V. These results agreed with the reports of Zhang et al (Zhang, Whistler, BeMiller, & Hamaker, 2005) and Jaiturong et al (Jaiturong, Laosirisathian, Sirithunyalug, Eitssayeam, Sirilun, Chaiyana, et al., 2020) who indicated that starch granules from various banana cultivars were all irregular in shape and

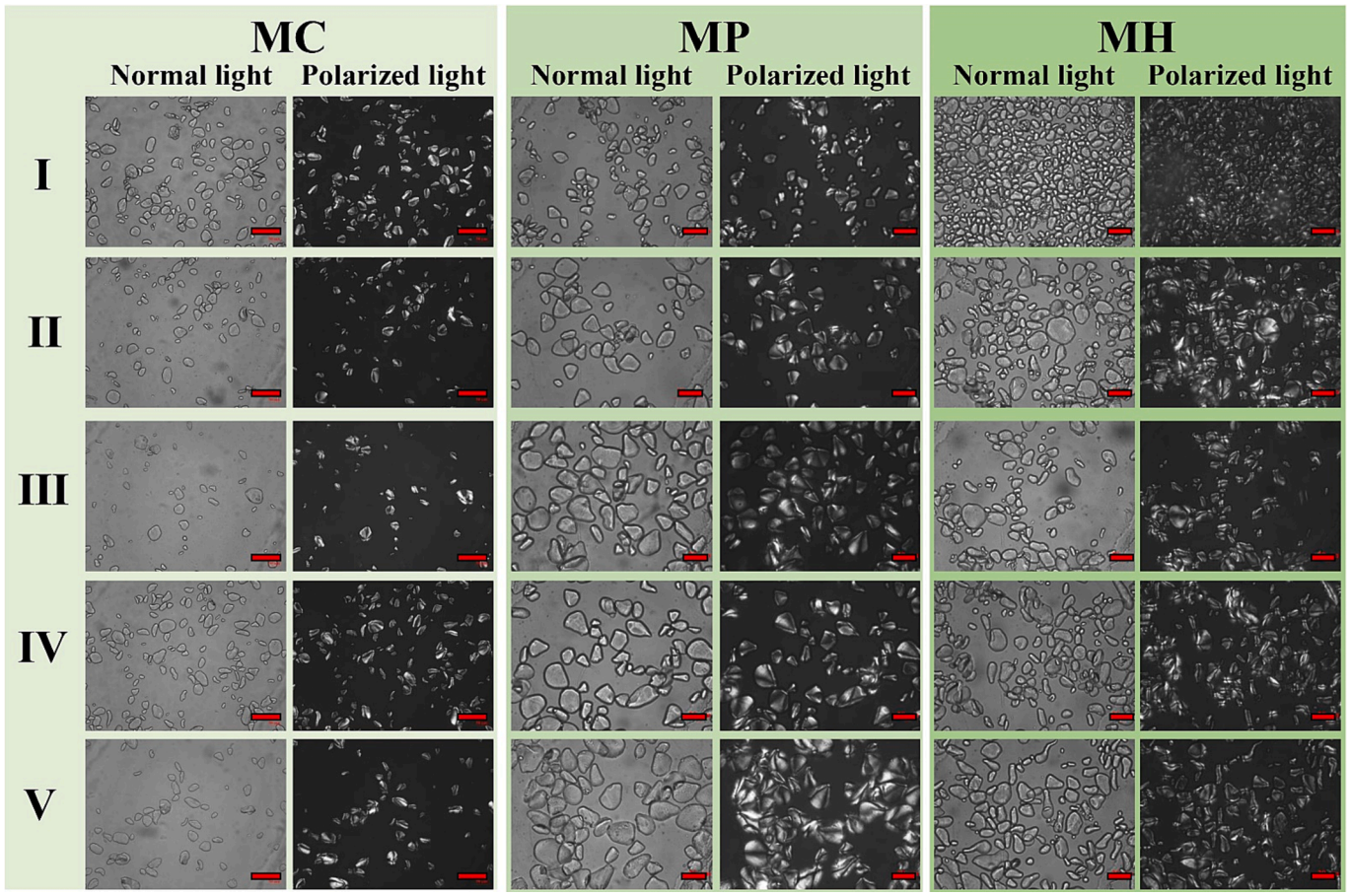

Fig. 1. Light microscopic images of MC, MP and MH starches at different maturity stages (I -V). Scale bar: 20 μm.

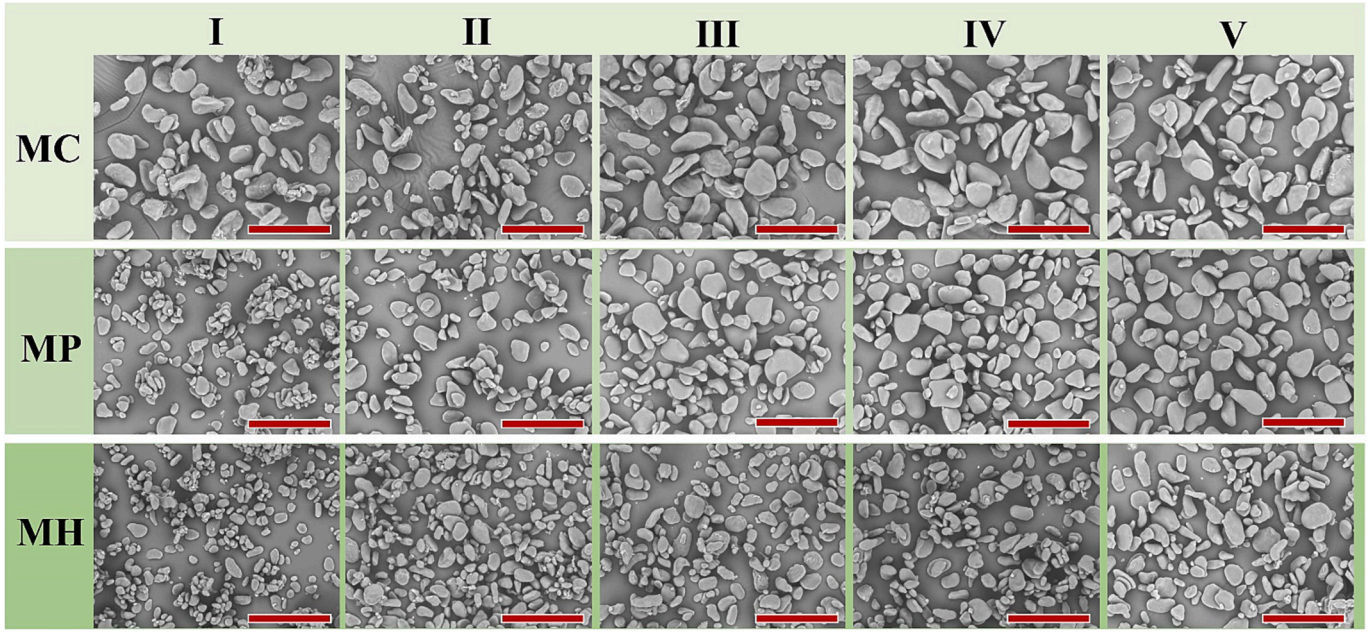

Fig. 2. Scanning electron microscopic images of MC, MP and MH starches at different maturity stages (I -V). Scale bar: 20 μm.

appeared in elongated and spheroid form. With respect to particle size, MC starch granules size did not obviously change before stage III, but increased noticeably at stage III and maintained at the same level afterwards. In comparison, the particle size of MP and MH starches gradually increased throughout the five stages. Collectively, these results suggest that the growth period has little effect on banana starch morphology.

Particle size distribution

The particle size distributions of the samples are shown in Table 1. The average diameter (*D* [4, 3]) of MC starch increased from 33.63 μm in stage I to 36.43 μm in stage IV, and then significantly increased to 54.10 μm in stage V, indicating that a fast growth occurred between stage IV and stage V. The *D* [4, 3] of MP starch gradually increased from 31.97 μm in stage I to 59.53 μm in stage V. The *D* [4, 3] of MH gradually increased from stage I to IV (from 33.62 μm to 58.11 μm), and significantly increased to 75.66 μm in stage V, which was similar to the growth pattern of MC particles. This result provides an interesting information that the average diameter of three BS granules increased with the fruit development of banana. The *D* [V, 0.1] indicates a value that 10 % of the overall particles show a size smaller than this value. As shown in Table 1, the *D* [V, 0.1] of MC starch increased with maturity. However, the *D* [V, 0.1] of the MH was barely changed with maturity. The *D* [V, 0.1], *D* [V, 0.5] and *D* [V, 0.9] of MC, MP and MH at stage V were overall higher than other stages, which supported that the starches at stage V had bigger granules. These results indicate that BS from different varieties have different dynamic pattern of morphology and particle size distribution, which are similar to previous findings that the size of BS granule depends on banana cultivar (Utrilla-Coello, Rodríguez-Huezo, Carrillo-Navas, Hernández-Jaimes, Vernon-Carter, & Alvarez-Ramirez, 2014).

Crystalline structure

XRD spectra of MC, MP, and MH starches are shown in Fig. 3. The MC and MH starch exhibited typical C-type crystalline pattern with reflection peaks centered at 5.5°, 15.3°, 17.1°, and 23.0° (2θ), which were consistent with the diffraction pattern of plantain (*Musa* ABB) starch (Bi, Zhang, Gu, Cheng, Li, Li, et al., 2019). However, characteristic peaks of MP starch appeared at 5.5°, 17.1°, 22.0°, and 24.0° (2θ), suggesting a B-type crystalline pattern, which has been suggested as the most frequently found crystalline structure in BS (Jaiturong, Laosirisathian, Sirithunyalug, Eitssayeam, Sirilun, Chaiyana, et al., 2020). The starches of the three varieties presented similar diffraction curves at all maturity stages, suggesting the same crystalline structure during growth. Therefore, the growth period does not affect the organization of the crystalline structure of BS.

The relative crystallinity of MC and MP starch slightly increased with maturity, whereas the relative crystallinity of MH starch showed higher increased (from 30.9 to 37.4 %) with maturity. MC starch had the lowest relative crystallinity, while MP and MH had similar relative crystallinity. An inversely correlated was between relative crystallinity with apparent amylose content. Chung et al (Chung, Liu, Lee, & Wei, 2011) also reported that the relative crystallinity of rice starches increased with a decrease in apparent amylose content. It was possible that amylopectin was a major component of the crystalline structure of starch, and amylose disrupted the crystalline build-up of amylopectin, resulting in high levels of amylose leading to a decrease in relative crystallinity.

Chemical structure

The FT-IR spectra of MC, MP, MH starches are presented in Fig. 4. All the starches demonstrated a similar profile. The absorption peak at 3461 cm^{-1} was associated with the free O—H bond stretching in glucose units (Hao, Chen, Li, & Gao, 2018). The absorption peak at 1645 cm^{-1} could spring from the bending vibration of O—H in tightly bound water (Chen, Hao, Ting, Li, & Gao, 2019). The peak at 989 cm^{-1} was due to the C—O bond stretching. The absorption peaks at 1156 cm^{-1}, 1083 cm^{-1}, and 1020 cm^{-1} could result from the stretching of glycosidic linkage (C—O—C), which makes up the backbone of starch chains.

The band at 1022 cm^{-1} is associated with vibrational modes within the amorphous domains of starch granules, and the decrease of its intensity is related to some increase of crystallinity (Capron, Robert, Colonna, Brogly, & Planchot, 2007). The spectra of MC and MH starches indicated that the band at 1022 cm^{-1} decreased with maturity, which accorded with the XRD results where increased crystallinity with maturity was found. The ratio of the band at 1047 cm^{-1} to the band at 1022 cm^{-1} in FT-IR spectra (1047/1022 cm^{-1}) can be used to quantify the degree of order of starch, and the ratio of the band at 995 cm^{-1} to the band at 1022 cm^{-1} (995/1022 cm^{-1}) reflects the degree of order of the helical structure in starch (Lopez-Rubio, Flanagan, Gilbert, & Gidley, 2010). Herein, the ratio of the band at 989 cm^{-1} to the band at 1022

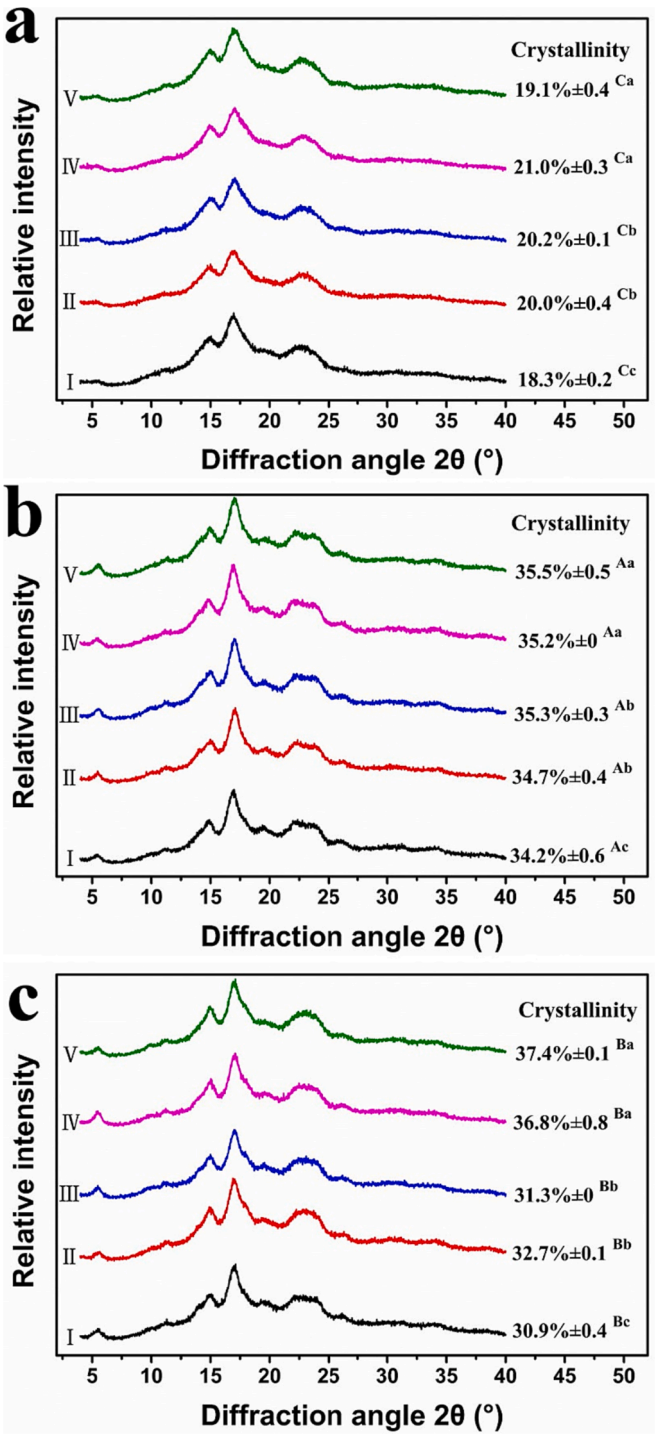

Fig. 3. The XRD spectra of MC (a), MP (b) and MH (c) starches at different maturity stages (I -V), in figure also demonstrated data on the relative crystallinity, data are expressed as the means ± SD. Values in the same column with different superscripts represent significant difference ($P < 0.05$). Upper case letters represent ANOVA for cultivars, lower case letters represent ANOVA for growth stages.

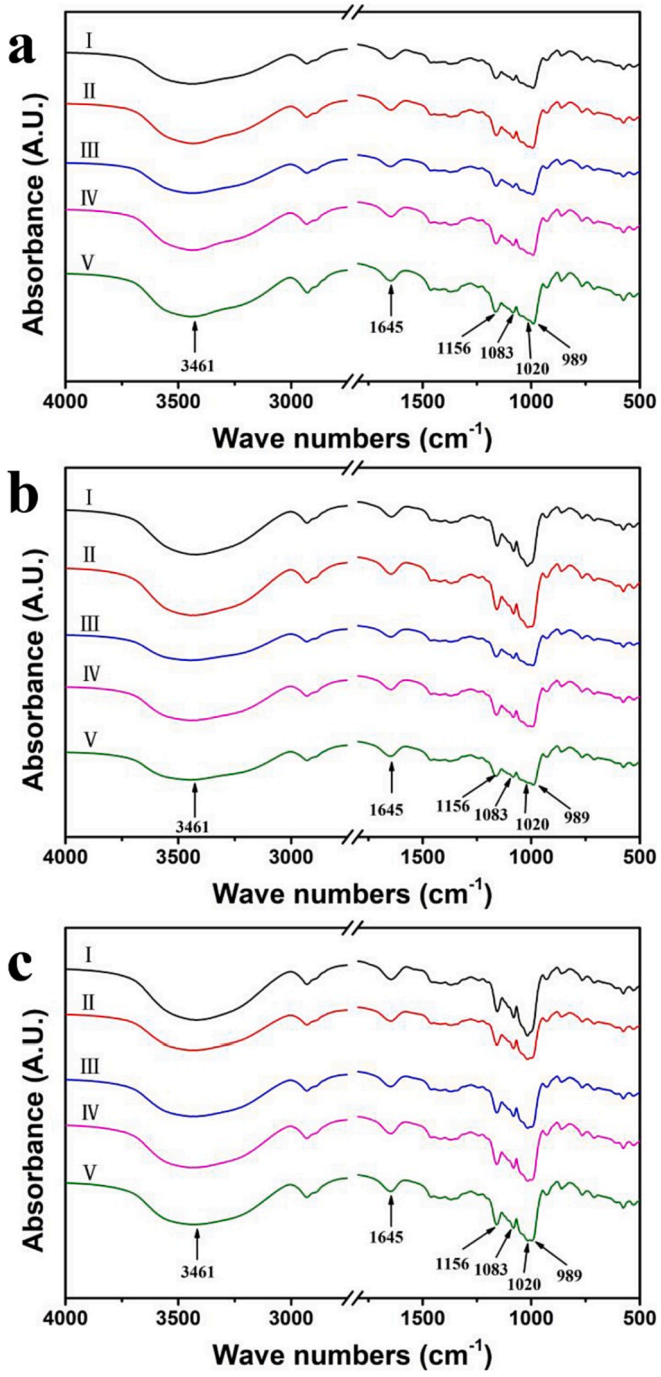

Fig. 4. FT-IR spectra of MC (a), MP (b) and MH (c) starches at different maturity stages (I -V).

cm^{-1} decreased in the FT-IR spectra of MP and MH starches since the alignment of double helices at short-range order was changed.

Thermal properties

The thermal parameters of MC, MP, and MH starches are shown in Table 2. T_o, T_p, and T_c showed a trend of first increasing, then dfenecreasing in MC cultivar, significantly decreased in MP cultivar, and no significant changes in MH cultivar as growth progressed. A previous study also reported the decreasing trend of T_o, T_p, and T_c during the growth period (Huang, Lin, & Wang, 2006; Liu, Weber, Currie, & Yada, 2003). Highly significant relationship ($r = 0.233$, $P < 0.05$) were found

Table 2
Differential scanning calorimetry results for the gelatinization of MC, MP and MH starches. Data are reported as mean ± S. D. ($n = 3$).

Starch samples		T_o (℃)[1]	T_p (℃)[1]	T_c (℃)[1]	ΔT(℃)[1]	ΔH (J/g)[2]
MC	I	74.22 ± 0.84 ^{Ba}	77.54 ± 1.14 ^{Ca}	84.05 ± 0.15 ^{Ab}	9.34 ± 0.49 ^{Aa}	13.83 ± 0.99 ^{Ab}
	II	75.44 ± 0.10 ^{Bb}	78.96 ± 0.25 ^{Ca}	87.00 ± 0.61 ^{Aa}	10.32 ± 0.37 ^{Aa}	18.72 ± 0.20 ^{Aa}
	III	76.45 ± 0.28 ^{Ba}	80.09 ± 0.40 ^{Ca}	86.43 ± 0.71 ^{Aa}	9.83 ± 0.33 ^{Aa}	16.73 ± 0.40 ^{Aa}
	IV	75.34 ± 0.11 ^{Bc}	79.08 ± 0.04 ^{Ca}	85.87 ± 1.03 ^{Aa}	11.20 ± 0.81 ^{Aa}	20.31 ± 1.90 ^{Aa}
	V	73.66 ± 0.05 ^{Bd}	77.50 ± 0.34 ^{Cb}	83.82 ± 0.66 ^{Aa}	11.93 ± 0.51 ^{Aa}	21.66 ± 2.03 ^{Aa}
MP	I	76.70 ± 0.60 ^{Ca}	79.54 ± 0.63 ^{Ba}	83.76 ± 1.31 ^{Cb}	7.06 ± 0.47 ^{Aa}	12.64 ± 0.52 ^{Bb}
	II	74.70 ± 0.26 ^{Cb}	78.34 ± 0.01 ^{Ba}	82.91 ± 0.21 ^{Ca}	8.21 ± 0.33 ^{Aa}	16.41 ± 0.76 ^{Ba}
	III	73.64 ± 1.96 ^{Ca}	77.89 ± 1.41 ^{Ba}	81.99 ± 1.57 ^{Ca}	8.35 ± 0.44 ^{Aa}	18.91 ± 0.52 ^{Ba}
	IV	73.50 ± 0.18 ^{Cc}	77.09 ± 0.20 ^{Ba}	82.22 ± 0.64 ^{Ca}	8.72 ± 0.58 ^{Aa}	20.74 ± 0.32 ^{Ba}
	V	71.09 ± 0.63^{Cd}	74.72 ± 0.53 ^{Bb}	79.55 ± 0.49 ^{Ca}	8.46 ± 0.10 ^{Aa}	13.86 ± 0.84 ^{Ba}
MH	I	76.44 ± 0.94 ^{Aa}	79.87 ± 0.93 ^{Aa}	84.34 ± 1.14 ^{Bb}	7.90 ± 0.14 ^{Aa}	9.77 ± 0.15 ^{Cb}
	II	76.08 ± 1.72 ^{Ab}	79.54 ± 1.94 ^{Aa}	85.58 ± 4.22 ^{Ba}	9.50 ± 1.77 ^{Aa}	11.20 ± 1.45 ^{Ca}
	III	76.25 ± 1.12 ^{Aa}	79.78 ± 1.26 ^{Aa}	85.53 ± 1.15 ^{Ba}	9.28 ± 0.02 ^{Aa}	14.67 ± 0.45 ^{Ca}
	IV	75.37 ± 0.08 ^{Ac}	79.06 ± 0.38 ^{Aa}	83.88 ± 1.18 ^{Ba}	8.51 ± 0.89 ^{Aa}	15.53 ± 0.47 ^{Ca}
	V	75.68 ± 2.84 ^{Ad}	80.39 ± 2.80 ^{Ab}	87.10 ± 3.90 ^{Ba}	11.42 ± 75 ^{Aa}	18.58 ± 0.84 ^{Ca}

Values in the same column with different letters are significantly different ($P < 0.05$). Upper case letters represent ANOVA for cultivars, lower case letters represent ANOVA for growth stages.[1] T_o, T_p, T_c, and ΔT indicate the onset, peak, conclusion, and gelatinization range temperature of gelatinization, respectively. [2] ΔH indicates enthalpy of gelatinization.

between peak gelatinization temperatures and starch apparent amylose content. Starch with a higher content of amylose content has a higher peak temperature because the starch granules have a higher resistance to swelling and require higher temperatures to leach out the amylose molecules and achieve maximum swelling (Park,Lbanez,Zhong & Shoemaker, 2007).

The ΔH of the three banana starches increased as growth progressed from stage I to stage V. For MC and MH cultivars demonstrated the highest gelatinization enthalpy at stage V, however highest gelatinization enthalpy values at stage IV for cultivar MP. *Trapa quadrispinosa* Roxb (Chiang, Li, Huang, & Wang, 2007) and taro (Himeda, Yanou, Nguimbou, Gaiani, & Mbofung, 2012) starches have shown similar behavior during their growth, while the potato starch exhibited the opposite tendency (Liu, Weber, Currie, & Yada, 2003). The high ΔH values at stage V indicate that the starch structures are more ordered. Furthermore, according to the correlation analysis, apparent amylose content in starches was positively correlated with gelatinization enthalpy ($r = 0.8$, $P < 0.01$). Similar trend was observed in the result of Aboubakar et al. (Aboubakar, Njintang, Scher, & Mbofung, 2008).

Pasting properties

Pasting characteristics of MC, MP, and MH starches are shown in Table 3. Although not significant, the T_p of all the starches decreased as growth progressed. MC, MP, and MH starches displayed a T_p of 74.0 °C, 76.0 °C, and 74.9 °C at stage V, respectively. This result was highly consistent with the report of Noda et al (Noda, Takahata, Sato, Hisamatsu, & Yamada, 1995) in yam, potato, and sweet potato starches during growth. The *Tp* was reached when the starch granules swell to

Table 3
Pasting characteristics of MC, MP and MH starches at different maturity stages (I-V). Data are reported as mean ± S. D. ($n = 3$).

Samples		T_p (°C)	η_{pk} (cP)	η_{sh} (cP)	η_{sc} (cP)	η_{ec} (cP)	η_f (cP)	η_{bd} (cP)	η_{sb} (cP)
MC	I	76.0 ± 1.2 ^{Aa}	120 ± 1^{Cd}	119 ± 1 ^{Ce}	106 ± 2^{Cd}	133 ± 2 ^{Ce}	147 ± 1^{Cd}	14 ± 1 ^{Ac}	27 ± 2^{Cd}
	II	75.5 ± 1.5 ^{Aa}	154 ± 3 ^{Cc}	150 ± 1 ^{Cc}	135 ± 2 ^{Cc}	181 ± 4 ^{Cc}	191 ± 1 ^{Cb}	19 ± 1 ^{Ab}	46 ± 1 ^{Cb}
	III	74.5 ± 3.2 ^{Aa}	124 ± 2 ^{Cc}	115 ± 3^{Cd}	93 ± 3 ^{Cc}	124 ± 2^{Cd}	144 ± 1 ^{Cc}	31 ± 2 ^{Ab}	31 ± 2 ^{Cc}
	IV	75.0 ± 2.0 ^{Aa}	115 ± 1 ^{Cb}	108 ± 2 ^{Cb}	85 ± 2 ^{Cb}	110 ± 1 ^{Cb}	127 ± 3 ^{Cb}	30 ± 1 ^{Aa}	25 ± 1 ^{Cb}
	V	74.0 ± 1.6 ^{Aa}	174 ± 2 ^{Ca}	169 ± 5 ^{Ca}	159 ± 1 ^{Ca}	213 ± 1 ^{Ca}	240 ± 2 ^{Ca}	15 ± 1 ^{Ab}	54 ± 2 ^{Ca}
MP	I	78.9 ± 0.8 ^{Aa}	145 ± 3 ^{Ad}	90 ± 3 ^{Be}	110 ± 1 ^{Bd}	149 ± 1 ^{Be}	198 ± 1 ^{Ad}	35 ± 2 ^{Bc}	39 ± 3 ^{Bd}
	II	78.3 ± 1.2 ^{Aa}	150 ± 3 ^{Ac}	99 ± 1 ^{Bc}	122 ± 1 ^{Bc}	167 ± 1 ^{Bc}	210 ± 3 ^{Ab}	28 ± 2 ^{Bb}	45 ± 3 ^{Bb}
	III	78.2 ± 2.2 ^{Aa}	160 ± 2 ^{Ac}	114 ± 2 ^{Bd}	156 ± 2 ^{Bc}	198 ± 1 ^{Bd}	208 ± 4 ^{Ac}	4 ± 1 ^{Bb}	42 ± 1 ^{Bc}
	IV	77.2 ± 4.1 ^{Aa}	195 ± 3 ^{Ab}	175 ± 4 ^{Bb}	175 ± 3 ^{Bb}	227 ± 1 ^{Bb}	243 ± 1 ^{Ab}	20 ± 2 ^{Ba}	52 ± 2 ^{Bb}
	V	76.0 ± 1.2 ^{Aa}	210 ± 4 ^{Aa}	191 ± 3 ^{Ba}	198 ± 2 ^{Ba}	237 ± 2 ^{Ba}	251 ± 2 ^{Aa}	12 ± 1 ^{Bb}	39 ± 1 ^{Ba}
MH	I	78.4 ± 0.4 ^{Aa}	122 ± 3 ^{Bd}	98 ± 2 ^{Ae}	122 ± 1 ^{Ad}	165 ± 3 ^{Ae}	168 ± 3 ^{Bd}	0	43 ± 2 ^{Ad}
	II	78.8 ± 1.6 ^{Aa}	145 ± 3 ^{Bc}	101 ± 5 ^{Ac}	145 ± 5 ^{Ac}	192 ± 4 ^{Ac}	192 ± 1 ^{Bb}	0	47 ± 2 ^{Ab}
	III	76.3 ± 2.9 ^{Aa}	162 ± 3 ^{Bc}	145 ± 1 ^{Ad}	157 ± 1 ^{Ac}	209 ± 1 ^{Ad}	205 ± 1 ^{Bc}	5 ± 1 ^{Cb}	52 ± 2 ^{Ac}
	IV	77.2 ± 4.1 ^{Aa}	178 ± 2 ^{Bb}	152 ± 1 ^{Ab}	170 ± 2 ^{Ab}	230 ± 2 ^{Ab}	220 ± 3 ^{Bb}	8 ± 2 ^{Ca}	60 ± 2 ^{Ab}
	V	74.9 ± 0.2 ^{Aa}	200 ± 5 ^{Ba}	192 ± 4 ^{Aa}	180 ± 7 ^{Aa}	233 ± 1 ^{Aa}	220 ± 3 ^{Ba}	20 ± 1 ^{Cb}	53 ± 3 ^{Aa}

Values followed by different superscript within a column differ significantly ($P < 0.05$). Upper case letters represent ANOVA for cultivars, lower case letters represent ANOVA for growth stages. T_p, pasting temperature; η_{pk}, peak viscosity; η_{sh}, viscosity at the start of the first holding temperature (95 °C); η_{sc}, viscosity at the start of cooling (95 °C); η_{ec}, viscosity at the end of cooling; η_f, final viscosity; η_{bd} (η_{pk} - η_{sc}), breakdown viscosity; η_{sb} (η_{ec} - η_{sc}), setback viscosity. The unit of viscosity is expressed as cP, which is obtained from the Modular Compact Rheometer.

their maximum volume, highly significant relationships were found between *Tp* and starch apparent amylose content (r = 0.461, $P < 0.01$). Because starch require a higher temperature to leach out the amylose molecules as they swell to their maximum.

The peak viscosity of the MP and MH starches increased from stage I to stage V. The peak viscosity at stage I was 120, 145, 122 cp for MC, MP, and MH, respectively, the peak viscosity at stage V was 174, 210, and 200 cp for MC, MP, and MH, respectively. The two observations were consistent with the report of Liu et al (Liu, Weber, Currie, & Yada, 2003) who found that potato starch granules displayed higher T_p and lower peak viscosity at stage I than other stages. A positive correlation (r = 0.369, P < 0.05) was observed between the apparent amylose content and peak viscosity. Lower peak viscosity indicated that the starch granules were more resistant to swelling, which was due to less leaching of the amylose starch and less swelling of the granules. This indicated that banana starch contains a high amount of shear resistant amylose starch or long straight chain starch side chains.

Interestingly, MP starches had the highest final viscosity compared to their counterparts at all stages, and all starches showed considerable breakdown changes as growth progressed. At the cooling stage, the viscosity of BS paste could increase rapidly due to the formation of numerous intermolecular hydrogen bonds (Leelavathi, Indrani, & Sidhu, 1987). Herein, the MC paste showed a higher setback at stage V, indicating that the MC starches had a higher retrogradation tendency with the growth. The value of setback correlates with the amount and molecular weight of the amylose starch precipitated in the granules and the residue of pasted starch (Woo, We, Kang, Shon, Chung, Yoon, et al., 2015). Moreover, many other factors, such as granule diameter (r = 0.759, $P < 0.01$), affect the pasting properties of starch (Zhao, Chen, Jin, Buwalda, Gruppen, & Schols, 2015).

In vitro digestibility

RDS, SDS, and RS contents of MC, MP, and MH starches are shown in Table 4. RS contents of MC and MP starches increased with maturity. Meanwhile, the RDS and SDS contents decreased from about 19.43 % to 12.71 % for MC and from 19.70 % to 14.84 % for MP from stage I to V. However, the RS contents of MH starches were barely changed as growth progressed, which were overall lower than that of MC and MP starches. The highest RS content was found in MC starch at stage V. Many studies have also shown that raw BS has high RS content (Wang et al., 2019; Zhang & Hamaker, 2012). The resistance of BS to enzymatic hydrolysis could originate from the smooth and dense surface. BS also have several blocklets that enhance enzyme action and reduce hydrolysis rates

Table 4
In vitro digestibility of MC, MP and MH starches at different maturity stages (I-V). Data are reported as mean ± S. D. ($n = 3$).

Samples		RDS (%)	SDS (%)	RS (%)
MC	I	2.56 ± 0.40 ^{Ca}	16.87 ± 0.22 ^{Aa}	80.57 ± 0.63 ^{Ac}
	II	3.34 ± 0.51 ^{Ca}	13.42 ± 2.16 ^{Ab}	83.23 ± 4.65 ^{Ab}
	III	3.37 ± 0.95 ^{Ca}	13.30 ± 1.98 ^{Ab}	83.32 ± 1.93 ^{Ab}
	IV	1.86 ± 0.06 ^{Ca}	9.20 ± 0.55 ^{Ab}	88.94 ± 0.60 ^{Aa}
	V	1.77 ± 0.34 ^{Cb}	10.94 ± 0.55 ^{Ac}	88.29 ± 0.21 ^{Aa}
MP	I	9.29 ± 0.05 ^{Aa}	10.41 ± 1.01 ^{Ba}	80.30 ± 0.52 ^{Bc}
	II	8.63 ± 0.24 ^{Aa}	10.16 ± 0.28 ^{Bb}	81.21 ± 0.14 ^{Bb}
	III	8.62 ± 0.37 ^{Aa}	10.20 ± 1.37 ^{Bb}	81.18 ± 1.07 ^{Bb}
	IV	8.31 ± 0.30 ^{Aa}	7.32 ± 0.26 ^{Bb}	84.37 ± 0.05 ^{Ba}
	V	7.40 ± 0.25 ^{Ab}	7.44 ± 0.51 ^{Bc}	85.16 ± 0.34 ^{Ba}
MH	I	6.60 ± 0.25 ^{Ba}	13.18 ± 0.01 ^{Aa}	80.22 ± 0.24 ^{Cc}
	II	6.90 ± 1.06 ^{Ba}	11.83 ± 0.39 ^{Ab}	81.27 ± 1.44 ^{Cb}
	III	7.48 ± 0.88 ^{Ba}	10.50 ± 1.94 ^{Ab}	82.02 ± 1.06 ^{Cb}
	IV	8.05 ± 0.06 ^{Ba}	10.51 ± 1.87 ^{Ab}	81.44 ± 1.80 ^{Ca}
	V	6.86 ± 0.49 ^{Bb}	12.69 ± 0.52 ^{Ac}	80.45 ± 1.01 ^{Ca}

Values in the same column with different letters (a-d) are significantly different ($P < 0.05$). Upper case letters represent ANOVA for cultivars, lower case letters represent ANOVA for growth stages.

Table 5
Relationship between apparent amylose content, D [4, 3], relative crystallinity, Tp, ΔT, ΔH, η_{pk}, η_f, η_{sb} and RS. r stands for Pearson's r, p for significance.

		apparent amylose content	RDS	SDS	RS
apparent amylose content	r		−0.387	−0.385	0.725
	P		0.009	0.009	0.000
D [4, 3]	r	0.398	0.147	−0.211	0.072
	P	0.007	0.336	0.164	0.639
relative crystallinity	r	−0.24	0.933	−0.48	−0.449
	P	0.112	0.000	0.001	0.002
T_p	r	0.233	0.008	0.352	−0.352
	P	0.014	0.959	0.018	0.018
ΔT	r	0.461	−0.619	0.316	0.265
	P	0.001	0.000	0.034	0.079
ΔH	r	0.8	−0.332	−0.248	0.547
	P	0.000	0.026	0.101	0.000
η_{pk}	r	0.369	0.43	−0.517	0.084
	P	0.013	0.003	0.000	0.585
η_f	r	0.197	0.525	−0.524	0.02
	P	0.194	0.000	0.000	0.896
η_{sb}	r	0.019	0.437	−0.246	−0.156
	P	0.903	0.003	0.103	0.307

(Zhang, Whistler, BeMiller, & Hamaker, 2005). A significant positive correlation ($r = 0.725$, $P < 0.01$) between the apparent amylose content and RS could be observed in our work (Table 5). This result indicated that starch containing more amylose was digested slower than starch with low amylose content. The same conclusion was obtained by Lopez-Silva et al. (Lopez-Silva, Bello-Perez, Castillo-Rodriguez, Agama-Acevedo, & Alvarez-Ramirez, 2020). This was mainly due to the fact that apparent amylose had more linear and flexible structures than amylopectin and were more resistant to amylase hydrolysis than amorphous starches. Herein, the digestibility of MC and MP was variance at different growth periods. However, a negative correlation between relative crystallinity and RS was observed in our work. The relative crystallinity of MH starch showed higher increased with growth progressed, this may be one of the reasons why MH's RS had remained the same. In addition to apparent amylose content and relative crystallinity, there were many other parameters (such as DP of the amylose, starch source, particle size, and crystallinity) that affect the enzyme digestibility of starch (You, Lim, Lee, & Chung, 2014). The DP of the apparent amylose in MH may be changed with growth progressed, as well as the surface morphology of MH was different from that of MC and MP, which may be another reason why MH's RS doesn't change with growth progressed.

Conclusions

In this study, the physiochemical properties and *in vitro* digestibility of BS from three cultivars at five different maturity stages were investigated. The apparent amylose content and particle size of all starches increased with maturity. Morphological characteristics of the starch granules varied with cultivar and maturity. The relative crystallinity of MC and MP starches, exhibiting C-type crystalline pattern, was not greatly changed, while that of MH starch, exhibiting B-type crystalline pattern, gradually increased during the ripening process. All starches showed similar chemical linkages in FT-IR spectra and were not affected by cultivar and maturity. Pasting property analysis indicated that the starches from different cultivars had different heat stability, cold stability, and setback at different maturity stages. In vitro digestion showed that all the banana starches possessed high RS contents. Moreover, the RS contents of MC and MP starches, but not MH starches, increased with maturity. In conclusion, all the three banana cultivars can provide RS. This study provides insights into using appropriate banana cultivars at suitable ripening stages for the production of RS related commercial products.

CRediT authorship contribution statement

Jiashui Wang: Conceptualization, Investigation, Formal analysis, Data curation, Validation, Visualization, Writing – original draft. **Yanxia Li:** Investigation, Formal analysis, Data curation. **Weihong Ma:** Formal analysis, Investigation. **Jiali Zhang:** Formal analysis, Investigation. **Hongbin Yang:** Formal analysis, Investigation. **Peicong Wu:** Formal analysis, Investigation. **Jingyang Li:** Formal analysis, Investigation. **Zhiqiang Jin:** Writing – review & editing, Project administration, Funding acquisition, Supervision.

Declaration of competing interest

The authors declare that they have no known competing financial interests or personal relationships that could have appeared to influence the work reported in this paper.

Acknowledgement

This work is supported by China Agriculture Research System of MOF and MARA (CARS-31-02 and CARS-31-03).

References

AACC, American Association of Cereal Chemists.. (1983). *Approved methods of the AACC (8th Methods)*. St Paul, MN: AACC.
Aboubakar, Njintang, Y. N., Scher, J., & Mbofung, C. M. F. (2008). Physicochemical, thermal properties and microstructure of six varieties of taro (Colocasia esculenta L. Schott) flours and starches. *Journal of Food Engineering, 86*(2), 294–305.
Baik, B. K., & Lee, M. R. (2003). Effects of starch amylose content of wheat on textural Properties of white salted noodles. *Cereal Chemistry, 80*(3), 304–309.
Bello-Pérez, L. A., Agama-Acevedo, E., Sánchez-Hernández, L., & Paredes-López, O. (1999). Isolation and partial characterization of banana starches. *Journal of Agricultural and Food Chemistry, 47*(3), 854–857.
Bi, Y., Zhang, Y., Gu, Z., Cheng, L., Li, Z., Li, C., & Hong, Y. (2019). Effect of ripening on in vitro digestibility and structural characteristics of plantain (Musa ABB) starch. *Food Hydrocolloids, 93*, 235–241.
Capron, I., Robert, P., Colonna, P., Brogly, M., & Planchot, V. (2007). Starch in rubbery and glassy states by FTIR spectroscopy. *Carbohydrate Polymers, 68*(2), 249–259.
Chen, Y., Hao, Y., Ting, K., Li, Q., & Gao, Q. (2019). Preparation and emulsification properties of dialdehyde starch nanoparticles. *Food Chemistry, 286*, 467–474.
Cheng, Y., Yang, G., Wang, J., Bing, D., Bao, J., Wen, S., & Ding, W. (2008). Effects of spray drying technologies on the retention rate of banana resistant starch. *Transactions of the Chinese Society of Agricultural Engineering, 24*(6), 282–286.
Chiang, P. Y., Li, P. H., Huang, C. C., & Wang, C. C. R. (2007). Changes in functional characteristics of starch during water caltrop (Trapa Quadrispinosa Roxb.) growth. *Food Chemistry, 104*(1), 376–382.
Chung, H. J., Liu, Q., Lee, L., & Wei, D. (2011). Relationship between the structure, physicochemical properties and *in vitro* digestibility of rice starches with different amylose contents. *Food Hydrocolloids, 25*(5), 968–975.
Das, M., Rajan, N., Biswas, P., & Banerjee, R. (2022). A novel approach for resistant starch production from green banana flour using amylopullulanase. *LWT - Food Science and Technology, 153*, Article 112391.
Englyst, H. N., Kingman, S. M., & Cummings, J. H. (1992). Classification and measurement of nutritionally important starch fractions. *European Journal of Clinical Nutrition, 46*(2), 33–50.
Gutiérrez, T. J., & Tovar, J. (2021). Update of the concept of type 5 resistant starch (RS5): Self-assembled starch V-type complexes. *Trends in Food Science & Technology, 109*, 711–724.
Hao, Y., Chen, Y., Li, Q., & Gao, Q. (2018). Preparation of starch nanocrystals through enzymatic pretreatment from waxy potato starch. *Carbohydrate Polymers, 184*, 171–177.
Himeda, M., Yanou, N. N., Nguimbou, R. M., Gaiani, C., & Mbofung, C. M. F. (2012). Physicochemical, rheological and thermal properties of taro (Colocassia esculenta) starch harvested at different maturity stages. *International Journal of Biosciences, 2*(3), 14–27.
Huang, C. C., Lin, M. C., & Wang, C. C. R. (2006). Changes in morphological, thermal and pasting properties of yam (Dioscorea alata) starch during growth. *Carbohydrate Polymers, 64*(4), 524–531.
Kaur, L., Dhull, S. B., Kumar, P., & Singh, A. (2020). Banana starch: Properties, description, and modified variations - A review. *International Journal of Biological Macromolecules, 165*, 2096–2102.
Leelavathi, K., Indrani, D., & Sidhu, J. S. (1987). Amylograph pasting behaviour of cereal and tuber starches. *Starch - Stärke, 39*(11), 378–381.
Liu, Q., Weber, E., Currie, V., & Yada, R. (2003). Physicochemical properties of starches during potato growth. *Carbohydrate Polymers, 51*(2), 213–221.
Lopez-Silva, M., Bello-Perez, L. A., Castillo-Rodriguez, V. M., Agama-Acevedo, E., & Alvarez-Ramirez, J. (2020). In vitro digestibility characteristics of octenyl succinic acid (OSA) modified starch with different amylose content. *Food Chemistry, 304*, Article 125434.
Lopez-Rubio, A., Flanagan, B. M., Gilbert, E. P., & Gidley, M. J. (2008). A novel approach for calculating starch crystallinity and its correlation with double helix content: A combined XRD and NMR study. *Biopolymers, 89*(9), 761–768.
Madsen, M. H., & Christensen, D. H. (1996). Changes in viscosity properties of potato starch during growth. *Starch-Stärke, 48*(7–8), 245–249.
Nara, S., Sakakura, M., & Komiya, T. (1983). On the acid resistance of starch granules. *Starch - Stärke, 35*(8), 266–270.
Noda, T., Takahata, Y., Sato, T., Hisamatsu, M., & Yamada, T. (1995). Physicochemical properties of starches extracted from sweet potato roots differing in physiological Age. *Journal of Agricultural and Food Chemistry, 43*(12), 3016–3020.
Noda, T., Tsuda, S., Mori, M., Takigawa, S., Matsuura-Endo, C., Saito, K., Arachichige Mangalika, W. H., Hanaoka, A., Suzuki, Y., & Yamauchi, H. (2004). The effect of harvest dates on the starch properties of various potato cultivars. *Food Chemistry, 86*(1), 119–125.
Park, I. M., Lbanez, A. M., Zhong, F., & Shoemaker, C. F. (2007). Gelatinization and pasting Properties of waxy and non-waxy rice starches. *Starch-Starke, 59*(8), 388–396.
Srikaeo, K., Mingyai, S., & Sopade, P. A. (2011). Physicochemical properties, resistant starch content and enzymatic digestibility of unripe banana, edible canna, taro flours and their rice noodle products. *International Journal of Food Science & Technology, 46*(10), 2111–2117.
Sivak, M. N., & Preiss, J. (1998). Physicochemical structure of the starch granule. *Advance Food Nutrition Research, 41*, 13–32.
Tan, X. Y., Gu, B., Li, X. X., Xie, C. F., Chen, L., & Zhang, B. J. (2017). Effect of growth period on the multi-scale structure and physicochemical properties of cassava starch. *International Journal of Biological Macromolecules, 101*, 9–15.
Thanyapanich, N., Jimtaisong, A., & Rawdkuen, S. Functional properties of banana starch (*Musa* spp.) and its utilization in cosmetics. *Molecules*, *26*(12), 3637.

Tie, P. L., Karim, A. A., & Manan, D. M. A. (2010). Physicochemical properties of starch in sago palms (Metroxylon sagu) at different growth stages. *Starch - Stärke, 60*(8), 408–416.

Tsai, C. Y., Salamini, F., & Nelson, O. E. (1970). Enzymes of carbohydrate metabolism in the developing endosperm of maize. *Plant Physiology, 46*(2), 299–306.

Utrilla-Coello, R. G., Rodríguez-Huezo, M. E., Carrillo-Navas, H., Hernández-Jaimes, C., Vernon-Carter, E. J., & Alvarez-Ramirez, J. (2014). *In vitro* digestibility, physicochemical, thermal and rheological properties of banana starches. *Carbohydrate Polymers, 101*, 154–162.

Wang, J. S., Wang, A. B., Ma, W. H., Xu, B. Y., Zang, X. P., Tan, L., Jin, Z. Q., & Li, J. Y. (2019). Comparison of physicochemical properties and *in vitro* digestibility of starches from seven banana cultivars in China. *International Journal of Biological Macromolecules, 121*, 279–284.

Wang, J., Tang, X. J., Chen, P. S., & Huang, H. H. (2014). Changes in resistant starch from two banana cultivars during postharvest storage. *Food Chemistry, 156*, 319–325.

Woo, H. D., We, G. J., Kang, T. Y., Shon, K. H., Chung, H. W., Yoon, M. R., Lee, J. S., & Ko, S. (2015). Physicochemical and gelatinization properties of starches separated from various rice cultivars. *Journal of Food Science, 80*(10), E2208–E2216.

You, S. Y., Lim, S. T., Lee, J. H., & Chung, H. J. (2014). Impact of molecular and crystalline structures on *in vitro* digestibility of waxy rice starches. *Carbohydrate Polymers, 112*, 729–735.

Zhang, P., & Hamaker, B. R. (2012). Banana starch structure and digestibility. *Carbohydrate Polymers, 87*(2), 1552–1558.

Zhang, P., Whistler, R. L., BeMiller, J. N., & Hamaker, B. R. (2005). Banana starch: Production, physicochemical properties, and digestibility - a review. *Carbohydrate Polymers, 59*(4), 443–458.

Zhao, J., Chen, Z., Jin, Z., Buwalda, P., Gruppen, H., & Schols, H. A. (2015). Effects of granule size of cross-linked and hydroxypropylated sweet potato starches on their physicochemical properties. *Journal of Agricultural and Food Chemistry, 63*(18), 4646–4654.